

# Principled model selection for stochastic dynamics

Andonis Gerardos and Pierre Ronceray\*

Aix Marseille Univ, CNRS, CINAM, Turing Center for Living Systems, Marseille, France

Complex dynamical systems, from macromolecules to ecosystems, are often modeled by stochastic differential equations. To learn such models from data, a common approach involves sparse selection among a large function library. However, we show that overfitting arises - not just from individual model complexity, but also from the combinatorial growth of possible models. To address this, we introduce Parsimonious Stochastic Inference (PASTIS), a principled method combining likelihood-estimation statistics with extreme value theory to suppress superfluous parameters. PASTIS outperforms existing methods and reliably identifies minimal models, even with low sampling rates or measurement error. It extends to stochastic partial differential equations, and applies to ecological networks and reaction-diffusion dynamics.

Data-driven approaches to physical modeling, which seek to derive governing equations directly from experimental data rather than from theoretical insight or bottom-up model construction, have been rapidly advancing [1]. They are of particular interest in the context of dynamical systems, where data are trajectories, whose temporal evolution is modeled by differential equations. We can distinguish different levels of ambition for such data-driven methods, ranging from the estimation of parameters of a known equation [2, 3], to the discovery of a minimal model among a large class of possible ones. For deterministic systems governed by ordinary or partial differential equations, the advent of symbolic regression [4, 5] and Sparse Identification of Nonlinear Dynamics (SINDy) [6, 7] has provided practical ways to perform such model discovery. In contrast, for stochastic dynamical systems, few attempts have been made [8–12]. Those that do exist often lack a solid theoretical foundation and rely on heuristic truncations and fine-tuning hyperparameters. In this work, we establish a rigorous theoretical framework grounded in extreme value statistics applied to model selection. This approach provides a principled way to compare models and helps guide the design of effective data-driven methodologies for stochastic systems.

We organize this paper as follows. Our starting point is a quasi-likelihood method, Stochastic Force Inference [13], to estimate SDE parameters. We first show how likelihood estimates must be corrected in order to fairly compare two models, resulting in Akaike’s information criterion (AIC) for SDEs. We then move to model selection from a library of basis functions, and show that AIC systematically fails to select the minimal model against the many more complex models due to multiple hypothesis testing. Our central result is a modified information criterion, Parsimonious Stochastic Inference (PASTIS), that combines exact results from likelihood estimation statistics and extreme value theory to select sparse SDE models. Importantly, PASTIS model selection accounts not only for the complexity of

a given model, but also for the complexity-dependent combinatorial number of possible models. Comparing this method to pre-existing ones, we demonstrate that it performs comparably well in the near-deterministic sector and is a significant improvement over the state of the art for strongly stochastic systems. We show that it straightforwardly extends to continuous fields modeled by stochastic partial differential equations. Finally, we demonstrate the robustness of the method to data imperfections (sampling rate and measurement error), as well as its applicability to models of experimental interest: the identification of interaction networks in multi-species ecosystem and of chemical reaction-diffusion pathways.

**Model class.** We focus here on Brownian dynamics, the most broadly used class of continuous stochastic dynamical model. Specifically, we consider a  $d$ -dimensional autonomous first-order stochastic differential equation,

$$\frac{d\mathbf{x}_t}{dt} = \mathbf{F}(\mathbf{x}_t) + \sqrt{2\mathbf{D}(\mathbf{x}_t)}\xi(t) \quad (1)$$

where the force field  $\mathbf{F}(\mathbf{x})$  (also called *drift*) characterizes the deterministic part of the dynamics, the diffusion matrix  $\mathbf{D}(\mathbf{x})$  is symmetric positive definite and characterizes the stochastic part, and  $\xi$  is a  $d$ -dimensional Gaussian white noise. Throughout, we interpret multiplicative noise in the Itô sense. Here we focus on the force field, which is generally the most physically informative part of the dynamics.

**Inference by linear regression.** Our goal is thus to reconstruct, from an observed time series  $\mathbf{X} = \{\mathbf{x}_t\}_{t=0, \Delta t, \dots, \tau}$ , an inferred force field  $\hat{\mathbf{F}}(\mathbf{x})$  that best approximates the true  $\mathbf{F}(\mathbf{x})$ . To this aim, we adopt a widely used method consisting in approximating the force as a linear combination of basis functions  $\mathcal{B} = \{\mathbf{b}_i(\mathbf{x})\}_{i=1..n_{\mathcal{B}}}$  with coefficients  $\hat{F}_i$ , such that the inferred drift field reads

$$\hat{\mathbf{F}}^{\mathcal{B}}(\mathbf{x}) = \sum_{i=1}^{n_{\mathcal{B}}} \hat{F}_i^{\mathcal{B}} \mathbf{b}_i(\mathbf{x}). \quad (2)$$

The inference problem thus decomposes into two parts: 1) selecting the basis functions  $\mathbf{b}_i(\mathbf{x})$ , which is the main focus of this article, and 2) inferring the corresponding coefficient values, for which we follow an approach closely related to Stochastic Force Inference [13] (SFI).

\* pierre.ronceray@univ-amu.fr

**Inferring coefficient values.** We first briefly summarize the SFI method. Our starting point is the following approximate log-likelihood function  $\mathcal{L}(\mathbf{X}|\bar{\mathbf{F}})$  for the trajectory  $\mathbf{X}$  in a test force field  $\bar{\mathbf{F}}$ :

$$\mathcal{L}(\mathbf{X}|\bar{\mathbf{F}}) = -\frac{\tau}{4} \left\langle \left( \frac{\Delta \mathbf{x}_t}{\Delta t} - \bar{\mathbf{F}}_t \right) \cdot \bar{\mathbf{D}}^{-1} \cdot \left( \frac{\Delta \mathbf{x}_t}{\Delta t} - \bar{\mathbf{F}}_t \right) \right\rangle \quad (3)$$

where  $\Delta \mathbf{x}_t = \mathbf{x}_{t+\Delta t} - \mathbf{x}_t$ ,  $\bar{\mathbf{F}}_t = \bar{\mathbf{F}}(\mathbf{x}_t)$ , and  $\langle \cdot \rangle = \frac{1}{\tau} \sum_t \cdot \Delta t$  denotes trajectory averaging, with  $\Delta t$  the time interval and  $\tau$  the total time. Here  $\bar{\mathbf{D}} = \frac{1}{2\Delta t} \langle \Delta \mathbf{x}_t \otimes \Delta \mathbf{x}_t \rangle$  is an estimate of the mean diffusion matrix. Importantly, when the dynamical noise is additive and with ideal data ( $\Delta t \rightarrow 0$ , no measurement error), we have  $\bar{\mathbf{D}} \rightarrow \mathbf{D}$ , and  $\mathcal{L}$  coincides with the log-likelihood of the data in the force field  $\bar{\mathbf{F}}$ , up to an  $\bar{\mathbf{F}}$ -independent constant [14]. In the general case of multiplicative dynamical noise, our approach remains practical, while true maximum likelihood is notoriously hard due to the difficulty of accurately estimating the state-dependent inverse diffusion matrix [15–17].

In practice, given a basis of functions  $\mathcal{B} = \{\mathbf{b}_i(\mathbf{x})\}_{i=1..n_{\mathcal{B}}}$ , one can easily maximize Eq. 3 to obtain the inferred force coefficients

$$\hat{F}_i^{\mathcal{B}} = \sum_j G_{\mathcal{B}}^{-1}{}_{ij} \left\langle \frac{\Delta \mathbf{x}_t}{\Delta t} \cdot \bar{\mathbf{D}}^{-1} \cdot \mathbf{b}_j(\mathbf{x}_t) \right\rangle \quad (4)$$

where  $(G_{\mathcal{B}})_{ij} = \langle \mathbf{b}_i(\mathbf{x}_t) \cdot \bar{\mathbf{D}}^{-1} \cdot \mathbf{b}_j(\mathbf{x}_t) \rangle$  is the Gram matrix associated to the basis  $\mathcal{B}$ . Note that in contrast with Ref. [13], we define basis functions as vector functions and fitting coefficients are scalars, which provides a more flexible and general framework for basis selection. Once the coefficients  $\hat{F}_i^{\mathcal{B}}$  are obtained, the force field can be reconstructed and extrapolated beyond the trajectory using Eq. 2. In line with [13], we can define the *information* captured by the basis  $\mathcal{B}$  as the log-likelihood gain of the inferred force field with the basis  $\mathcal{B}$  compared to the null model with an empty basis (*i.e.* pure Brownian motion with zero force),

$$\mathcal{I}(\mathcal{B}) = \mathcal{L}(\mathbf{X}|\hat{\mathbf{F}}^{\mathcal{B}}) - \mathcal{L}(\mathbf{X}|0). \quad (5)$$

This information, which can be evaluated from data only, serves as a starting point to estimate the quality of the fit with the basis  $\mathcal{B}$ .

**Comparing bases.** We now turn to the main question of this article: how to compare and select the basis functions for stochastic inference? To decide which of two bases is best adapted to represent the data, it is not sufficient to compare the corresponding values of the information  $\mathcal{I}$ . Indeed, in this framework, given a basis  $\mathcal{B}$ , the same data is used to estimate the force parameters  $\hat{F}_i^{\mathcal{B}}$  and to evaluate the approximate likelihood  $\mathcal{L}(\mathbf{X}|\hat{\mathbf{F}}^{\mathcal{B}})$ . This data reuse biases the likelihood estimation towards selecting a model that overfits: bases with more functions are favored, even when they lead to larger error. To overcome this, we aim to minimize the mean squared error between the inferred and the true force along the data, which we can define as

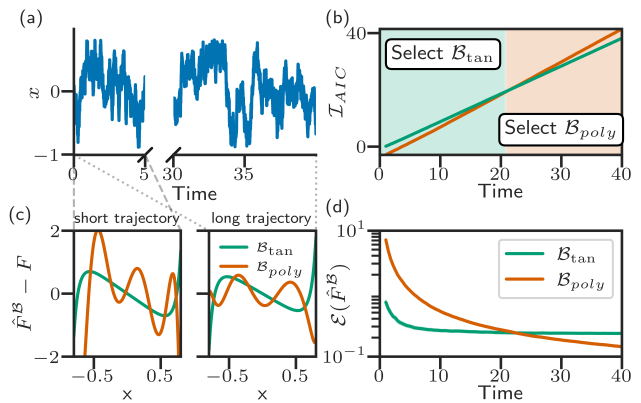


FIG. 1. **Comparing models using AIC.** (a) Simulated trajectory of a one-dimensional toy model with force  $F(x) = \frac{-x}{(1-x^2)^2}$  and dynamical noise  $D = 0.4$ . (b)  $\mathcal{I}_{AIC}$  as a function of total time for two bases: a single-parameter one  $\mathcal{B}_{tan} = \{\tan(x)\}$ , and an order-8 polynomial  $\mathcal{B}_{poly} = \{x^k\}_{k=0..8}$ . (c) Inferred force minus true force along the trajectory, for each basis and for a short and a long trajectory. (d) Mean-squared error  $\mathcal{E}$  between true and inferred force *vs* total time.

$\mathcal{E}(\hat{\mathbf{F}}^{\mathcal{B}}) = \frac{1}{4} \left\langle \left( \mathbf{F} - \hat{\mathbf{F}}^{\mathcal{B}} \right) \cdot \bar{\mathbf{D}}^{-1} \cdot \left( \mathbf{F} - \hat{\mathbf{F}}^{\mathcal{B}} \right) \right\rangle$ . Although this error  $\mathcal{E}$  is not accessible without knowing the true force  $\mathbf{F}$ , is it possible to estimate *differences* of error between two bases  $\mathcal{B}$  and  $\mathcal{C}$  in an unbiased way:

$$\mathbb{E}[\mathcal{I}(\mathcal{C}) - \mathcal{I}(\mathcal{B})] \approx \tau \mathbb{E} \left[ \mathcal{E}(\hat{\mathbf{F}}^{\mathcal{B}}) - \mathcal{E}(\hat{\mathbf{F}}^{\mathcal{C}}) \right] + n_{\mathcal{C}} - n_{\mathcal{B}} \quad (6)$$

where  $\mathbb{E}$  indicates expectation value over trajectory ensembles,  $n_{\mathcal{B}}$  (resp.  $n_{\mathcal{C}}$ ) is the number of functions in the basis  $\mathcal{B}$  (resp.  $\mathcal{C}$ ), and we give a precise meaning to this approximation in Appendix 1. The constant terms  $n_{\mathcal{B}}$  and  $n_{\mathcal{C}}$  stem from noise correlations between coefficient inference and likelihood estimation: each coefficient in the model induces a constant unit bias in the measured information  $\mathcal{I}$ , characteristic of overfitting.

**Akaike's information criterion.** In order to compare models, we can correct the bias in Eq. 6 by defining  $\mathcal{I}_{AIC}(\mathcal{B}) = \mathcal{I}(\mathcal{B}) - n_{\mathcal{B}}$ . This quantity coincides, up to a factor  $-2$ , with the Akaike Information criterion [18], a classic statistical estimator of model quality. On average, models with higher  $\mathcal{I}_{AIC}$  have a lower inference error along the trajectory: in particular, if  $\mathcal{I}_{AIC}(\mathcal{B}) < 0$ , the model primarily fits the noise and a null model with zero force would provide a better fit. As a practical example, in Fig. 1, we consider the inference of a force field in one dimension with two possible bases:  $\mathcal{B}_{tan}$ , with a single parameter that provides a simple but imperfect fit, and  $\mathcal{B}_{poly}$  with many parameters and which can provide a better fit. When the amount of data is low, we find that  $\mathcal{I}_{AIC}(\mathcal{B}_{tan}) > \mathcal{I}_{AIC}(\mathcal{B}_{poly})$  as the complex model overfits the data (Fig. 1b). In contrast, for large amounts of data, the complex model provides a better fit and  $\mathcal{I}_{AIC}(\mathcal{B}_{tan}) < \mathcal{I}_{AIC}(\mathcal{B}_{poly})$ . Importantly, we confirm that the crossover between these two regimes coincides with

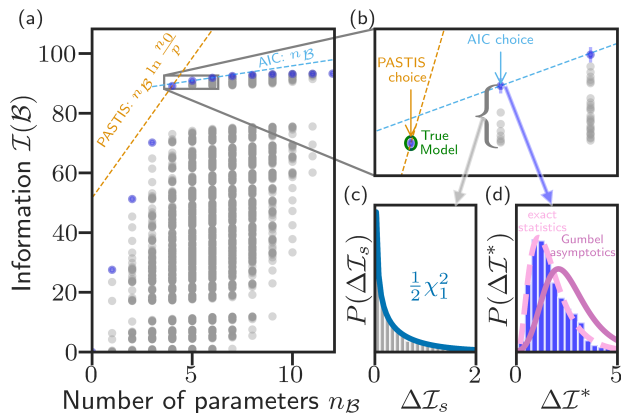


FIG. 2. **Information statistics of sparse models.** (a)  $\mathcal{I}(\mathcal{B})$  versus  $n_{\mathcal{B}}$  for all sub-models  $\mathcal{B} \subset \mathcal{B}_0 = \{1\mathbf{e}_1, \dots, x_3\mathbf{e}_3\}$  (with  $\mathbf{e}_i$  the unit vectors) of a 3-dimensional Ornstein-Uhlenbeck model with  $n^* = 4$  non-zero terms. The blue dots indicate the average  $\mathcal{I}$  of the top-ranked model of size  $n_{\mathcal{B}}$  across simulations, while gray dots correspond to the second, third, and lower-ranked models of size  $n_{\mathcal{B}}$  across simulations. Dashed lines represent the slopes of the penalization terms for AIC and PASTIS, intersecting at the point corresponding to the selected model. (b) Close-up on (a), showing that AIC selects models with superfluous parameters, while PASTIS correctly identifies the true model  $\mathcal{B}^*$ . (c) The distribution of the information gains  $\Delta\mathcal{I}_s$  for the true model + one superfluous term (histogram) is well captured by a  $\chi_1^2$  distribution (solid line). (d) The maximum  $\Delta\mathcal{I}^*$  of the information gain for one superfluous term  $\Delta\mathcal{I}_s$  is well captured by analytical extreme values theory (dashed line) and converges to the Gumbel distribution (Eq. 8) when  $n_0 \rightarrow \infty$  (Appendix 2).

the crossover in the actual inference error  $\mathcal{E}$  (Fig. 1b,d). Thus, AIC model selection, which consists in choosing the model with the maximal  $\mathcal{I}_{\text{AIC}}$ , estimated from data only, results in minimizing the true error  $\mathcal{E}$ .

**Sparse model selection.** When looking for a model without *a priori* basis, a common technique is to start with a large yet finite library  $\mathcal{B}_0$  of  $n_0 - n^*$  potential basis functions, such as polynomials, Fourier modes, exponentials, wavelets, etc. To avoid overfitting and permit model interpretation, such a library must then be reduced to a simpler basis  $\mathcal{B} \subset \mathcal{B}_0$  by eliminating most of the functions – *i.e.* by obtaining a sparse vector of coefficients  $\hat{F}_t^{\mathcal{B}_0}$  in the basis  $\mathcal{B}_0$ . This reduction thus consists, in practice, in attempting to identify the simplest model that best captures the data among the  $2^{n_0}$  possible combinations of basis functions in the library. To do so, we propose to define an *information criterion* allowing us to compare these many models, and to search among the possible models the one that maximizes this information criterion. Importantly, while AIC provides an unbiased way of comparing two models, it is not appropriate when comparing many models simultaneously.

**Failure of AIC.** Indeed, let us consider the case when there exists a true model  $\mathcal{B}^* \subset \mathcal{B}_0$  containing  $n^*$  functions that perfectly describe the system’s dynamics. We

define the *exact match accuracy* as the ensemble probability that this exact model is recovered by maximizing the chosen information criterion among all models. We find that with AIC, even in the limit of long trajectories, this accuracy does not converge to 100%: more complex models are selected, with superfluous terms, as illustrated in Fig. 2a-b. This reflects a well-known limitation of AIC [19]: it is not stringent enough to select the minimal or true model. To understand this, let us consider models consisting of the exact model plus one superfluous basis function,  $\mathcal{B}^* + \{s\}$  for  $s \in \mathcal{B}_0 - \mathcal{B}^*$ . According to Wilks’ theorem [20], under regularity conditions and as the observation time  $\tau \rightarrow \infty$ , the difference in the estimated log-likelihood value between  $\mathcal{B}^* + \{s\}$  and  $\mathcal{B}^*$  asymptotically follows a chi-squared distribution with one degree of freedom:

$$\Delta\mathcal{I}_s = \mathcal{I}(\mathcal{B}^* + \{s\}) - \mathcal{I}(\mathcal{B}^*) \sim \frac{1}{2}\chi_1^2. \quad (7)$$

This is indeed observed in practice (Fig. 2c). Thus  $\mathbb{E}[\Delta\mathcal{I}_{\text{AIC},s}] = \mathbb{E}[\Delta\mathcal{I}_s] - 1 = -\frac{1}{2}$ : superfluous terms reduce the AIC value and tend to be eliminated on average. However, for a given superfluous term, there is a non-vanishing probability  $P(\Delta\mathcal{I}_{\text{AIC},s} > 0) \approx 0.157$  that the AIC difference is positive even in the limit of large data sets. When the number of possible superfluous terms is large, the probability that one of them has an  $\mathcal{I}_{\text{AIC}}$  larger than that of  $\mathcal{B}^*$  goes to one, hence the systematic failure of AIC to identify the true model (Fig. 2a-b).

**Extreme value statistics of the information.** Crucially, to identify the true model  $\mathcal{B}^*$ , we need to distinguish it from *all* models with one superfluous term – and in particular the one with the highest likelihood. We thus need to study the statistics of the information gap  $\Delta\mathcal{I}^* = \max_{s \in \mathcal{B}_0 - \mathcal{B}^*} \Delta\mathcal{I}_s$  between the true model and the  $n_0 - n^*$  models with one superfluous term. This extreme value problem can be tackled by assuming independence of the  $\Delta\mathcal{I}_s$ , *i.e.* that  $\langle s(\mathbf{x}_t)s'(\mathbf{x}_t) \rangle = 0$  for superfluous functions  $s \neq s'$ . Under this assumption and using the Fisher-Tippett-Gnedenko theorem, the asymptotic behavior for large  $n_0 - n^*$  is  $\Delta\mathcal{I}^* \approx \log(n_0 - n^*) + Z$ , where  $Z \sim \text{Gumbel}(\mu = 0, \beta = 1)$  is a standard Gumbel random variable (Appendix 2). Using the properties of this distribution, we have

$$\mathbb{P}[\Delta\mathcal{I}^* < \log(n_0 - n^*) + z] \approx e^{-e^{-z}} \quad (8)$$

In practice, when  $n_0 - n^*$  is finite, the Gumbel approximation results in an overestimation of  $\Delta\mathcal{I}^*$  (Fig. 2d, Appendix 3).

**Information criterion for large bases.** Using these insights, we propose a modified information criterion, *Parsimonious Stochastic Inference* (PASTIS), that includes the effect of extreme value statistics due to large libraries of functions:

$$\mathcal{I}_{\text{PASTIS}}(\mathcal{B}) = \mathcal{I}(\mathcal{B}) - n_{\mathcal{B}} \log \frac{n_0}{p} \quad (9)$$

where  $p \ll 1$  is a user-chosen parameter setting the target probability of including a superfluous term in the model:

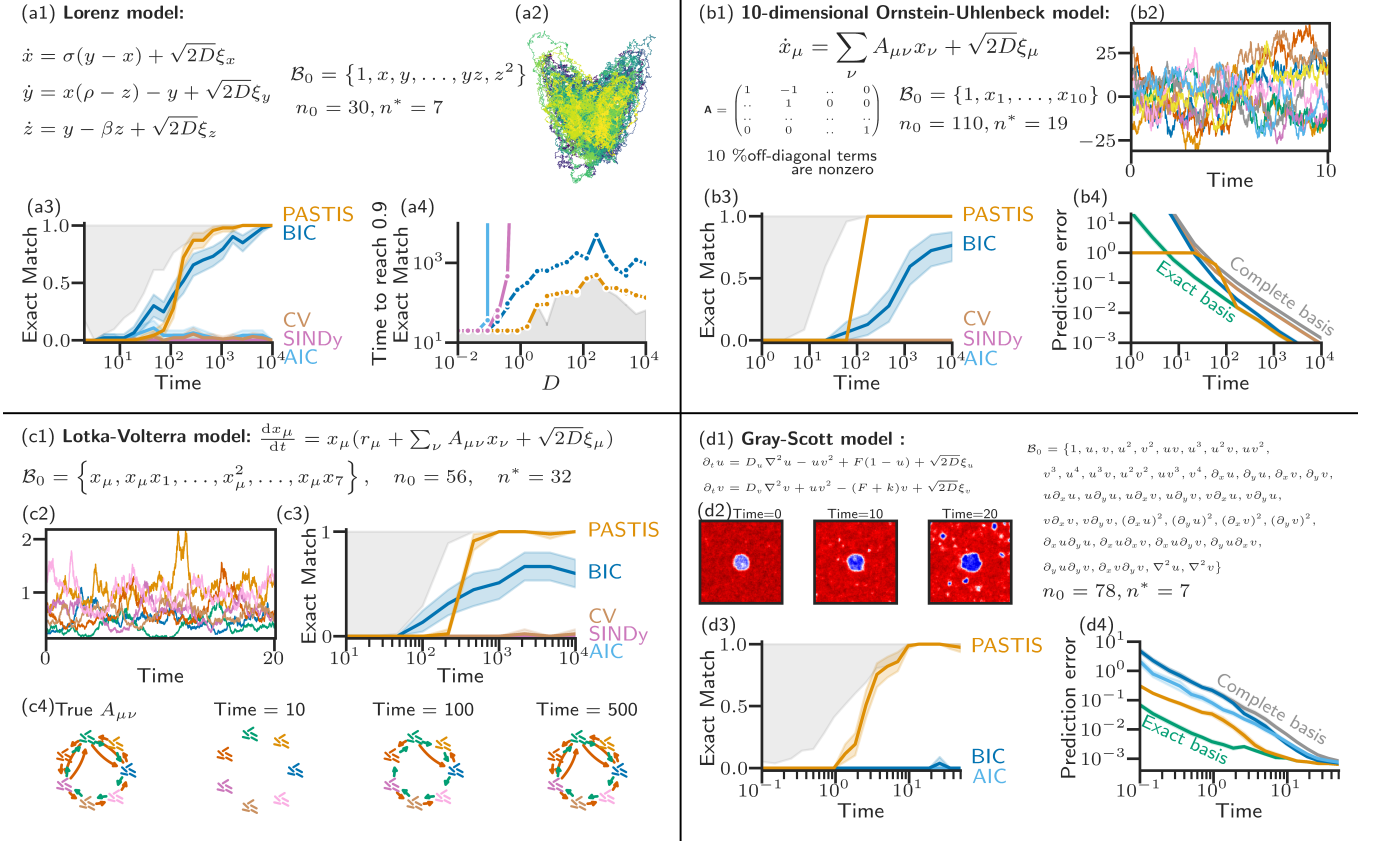


FIG. 3. **Benchmarking PASTIS.** For the four models considered (a-d), we indicate (1) the generating equation and fitting basis  $\mathcal{B}_0$  (each scalar function is considered along every unit vector), (2) a sample trajectory, and (3) the exact match accuracy as a function of total time for different sparsity-enforcing algorithms. The gray area indicates cases when the true model does not maximize  $\mathcal{I}$  between models with  $n^*$  parameters. (a4): Trajectory time necessary to obtain 90% exact match accuracy as a function of the Lorenz diffusion coefficient. (b4,d4): Prediction error of the inferred model for different algorithms, defined as  $\mathcal{E}(\hat{\mathbf{F}}^B)/\langle \mathbf{F} \cdot (4\bar{\mathbf{D}})^{-1} \cdot \mathbf{F} \rangle$  computed on an independent, asymptotically long trajectory. (c4): True interaction network and reconstructed network as a function of time using PASTIS, for a sparse stochastic Lotka-Volterra model with environmental noise. All curves are averages over 48 simulations. Simulation details in Appendix 7.

using Eq. 8, we have that  $\mathbb{P}[\max_s \mathcal{I}_{\text{PASTIS}}(\mathcal{B}^* + \{s\}) > \mathcal{I}_{\text{PASTIS}}(\mathcal{B}^*)] \approx p$  (details in Appendix 3). The multiple approximations made in the derivation of this criterion – estimated value for  $\bar{\mathbf{D}}$ , orthogonality of basis functions, use of  $n_0$  rather than  $n_0 - n_B$  in Eq. 9, Gumbel distribution – all go in the direction of parsimony, *i.e.* of overestimating the overfitting probability. In practice, we choose here  $p = 0.001$ . Lowering this value will lower the probability of overfitting, at the cost of needing more data to identify all nonzero coefficients in  $\mathcal{B}_0$ . The originality of  $\mathcal{I}_{\text{PASTIS}}$  is the fact that it explicitly accounts, in a principled way, for the size  $n_0$  of the initial basis: the complexity-dependent penalty to select a sparse model should not only account for the model size  $n_B$ , but also for the size of the model space that we consider.

**Exploring Model Space.** To find the true model, we need to maximize  $\mathcal{I}_{\text{PASTIS}}$  over the  $2^{n_0}$  models that can be constructed from the library  $\mathcal{B}_0$ . This non-convex optimization is, in general, a hard (NP-complete) problem that cannot be tackled exactly. However, we find that a

greedy hill-climbing algorithm with multiple initial points performs well and efficiently for this problem. Starting from an initial model, we randomly sample possible new models obtained by adding or removing a single parameter. When a model with higher  $\mathcal{I}_{\text{PASTIS}}$  is found, the move is accepted, until no further improvement is possible. We run multiple parallel searches, initialized with the null model, the complete model  $\mathcal{B}$ , and  $n_0$  randomly sampled models. We find that when the true model does indeed maximize  $\mathcal{I}_{\text{PASTIS}}$ , and it is recovered rapidly by this algorithm. It is computationally efficient, with each step requiring only the inversion of the matrix  $\mathbf{G}$  (Eq. 4): for instance, the identification of a model with  $n^* = 19$  terms in a basis with  $n_0 = 110$  functions can be reliably performed on a single CPU core in  $\approx 12$ s.

**Benchmarking PASTIS.** We use synthetic data on four models to demonstrate the efficiency of this method: the stochastic Lorenz model (Fig. 3a), a high-dimensional Ornstein-Uhlenbeck model with sparse coefficients (Fig. 3b), a generalized Lotka-Volterra model



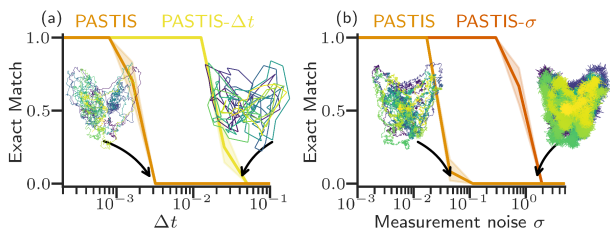


FIG. 4. **Robustness of PASTIS.** (a) Exact match accuracy with and without trapezoid modification for large time intervals  $\Delta t$ , for the Lorenz model with long trajectories ( $\tau = 4 \times 10^4$ ). (b) Same for the Stratonovich modification for measurement noise. Here  $x_t \rightarrow x_t + \eta$  where  $\eta \sim \mathcal{N}(0, \sigma^2)$ .

with multiplicative environmental noise and a sparse interaction network between species (Fig. 3c), and a noisy Gray-Scott model for spatial reaction-diffusion dynamics (Fig. 3d). In the first three cases, we use polynomial bases of first (b) and second (a,c) order. In Fig. 3d, we consider a stochastic partial differential equation model, which we treat by enriching the basis with discretized differential operators, and consider all terms up to second-order derivatives and fourth order in the variables  $u$  and  $v$ . We find that, in all cases, with sufficient amounts of data, the exact match accuracy of PASTIS converges to a value  $> 1 - p$  (Figs. 3a3-d3). This criterion is near-optimal: in most cases where it fails to identify the true model, it is because another model with the same number of parameters has higher estimated likelihood (gray area in all panels of Fig. 3), making the identification of  $\mathcal{B}^*$  essentially impossible.

**Comparing to other methods.** We perform a quantitative comparison of PASTIS with several other approaches. AIC, as expected from previous arguments, never converges for large bases. 7-fold Cross-Validation (CV), where the trajectory is split between 6 disjoint training sets for force coefficients inference and 1 testing set for likelihood evaluation, presents the same flaws as AIC. In contrast, the Bayesian Information Criterion (BIC) [21–23] that we adapted to SDE model selection (details in Appendix 4), with  $\mathcal{I}_{\text{BIC}}(\mathcal{B}) = \mathcal{I}(\mathcal{B}) - \frac{n\#}{2} \log \tau$ , does converge to the true model at large times, although much more slowly than PASTIS: indeed, the penalty increases with total time  $\tau$ . Finally, the py-SINDy [24] implementation of Sparse Identification of Nonlinear Dynamics [6] for ODEs shows performance similar to PASTIS in the near-deterministic level (Fig. 3a4, STLSQ, threshold = 0.5), but fails when the model becomes stochastic.

**Data imperfection.** In Fig. 3, we consider the total trajectory time as the only limitation of the data. However, experimental data has a finite, possibly large sampling interval  $\Delta t$ , as well as random measurement error on the values of  $\mathbf{x}_t$ . These imperfections incur biases both on the likelihood (Eq. 3) and on the inferred force coefficients (Eq. 4). While a complete treatment of the com-

bined effects of these two bias sources remains to be done, two simple insights can significantly improve PASTIS: a trapezoid integration rule [25, 26] for the inferred coefficient and estimated information and a robust diffusion estimator for large sampling interval (PASTIS- $\Delta t$  in Fig. 4a), and a Stratonovich representation of stochastic integrals similar to [13] for the inferred coefficient and estimated information combined to robust diffusion estimators [27] for measurement noise (PASTIS- $\sigma$  in Fig. 4b). We give further details and explicit corresponding formulas in Appendix 5.

**Discussion.** In this article, we studied quasi-likelihood maximization approaches to sparse inference of minimal models of stochastic differential equations from data. Existing methods typically rely either on arbitrary coefficient thresholding [6, 8, 24, 28] or penalization [29, 30], or on empirical assessment of statistical significance [13, 25, 31, 32]. In contrast, here we explicitly take into account the fact that selecting a simple model in a large basis of functions involves testing a large number of hypotheses, and thus the basis size should appear in sparsity-enforcing penalization. Leveraging exact results in likelihood estimation (Wilks’ theorem, Eq. 7) and extreme value statistics (Fisher-Tippett-Gnedenko theorem, Eq. 8), we derived a principled information criterion, Parsimonious Stochastic Inference (PASTIS, Eq. 9) for sparse model selection. The only tuning parameter,  $p$ , is directly interpretable as the target probability of adding a superfluous term. While we have kept this parameter fixed here, it could be made adaptive to both converge at long times and more efficiently fit at short times. We showed that this method is robust and efficient, including in high dimension, in the presence of dynamical noise, measurement error, and large time intervals. The inclusion of differential operators in the basis also permits the inference of stochastic partial differential equations from discretized fields, for which few inference methods pre-exist [33]. This work thus paves the way towards direct inference of minimal models from experimental trajectories, for instance to identify biochemical pathways, ecological networks (Fig. 3c) or reaction-diffusion mechanisms (Fig. 3d). Our information criterion can be seen as an extension of the classic Akaike information criterion [34, 35] to likelihood-based sparse selection of a minimal model, and could thus be applied to higher-order SDEs [32, 36, 37] as well as more general sparse modeling problems [38].

## ACKNOWLEDGMENTS

**Acknowledgments.** We warmly thank Thierry Mora, Anna Frishman, Nicolas Levernier, Simon Gsell, Martin Lardy and João Valeriano for precious advice. We acknowledge helpful input from ChatGPT. The project leading to this publication has received funding from France 2030, the French Government program managed by the French National Research Agency (ANR-

16-CONV-0001) and from Excellence Initiative of Aix-Marseille University - A\*MIDEX. PR thanks ICTP-

SAIFR (FAPESP grant 2021/14335-0) where part of this work was done. Co-funded by the European Union (ERC-SuperStoc-101117322).

- 
- [1] J. S. North, C. K. Wikle, and E. M. Schliep, A Review of Data-Driven Discovery for Dynamic Systems, *International Statistical Review* **91**, 464 (2023).
- [2] M. Bär, R. Hegger, and H. Kantz, Fitting partial differential equations to space-time dynamics, *Physical Review E* **59**, 337 (1999).
- [3] J. O. Ramsay, G. Hooker, D. Campbell, and J. Cao, Parameter Estimation for Differential Equations: A Generalized Smoothing Approach, *Journal of the Royal Statistical Society. Series B (Statistical Methodology)* **69**, 741 (2007), 4623296.
- [4] M. Schmidt and H. Lipson, Distilling Free-Form Natural Laws from Experimental Data, *Science* **324**, 81 (2009).
- [5] M. Cranmer, A. Sanchez-Gonzalez, P. Battaglia, R. Xu, K. Cranmer, D. Spergel, and S. Ho, Discovering Symbolic Models from Deep Learning with Inductive Biases (2020), arXiv:2006.11287 [astro-ph, physics:physics, stat].
- [6] S. L. Brunton, J. L. Proctor, and J. N. Kutz, Discovering governing equations from data by sparse identification of nonlinear dynamical systems, *Proceedings of the National Academy of Sciences* **113**, 3932 (2016).
- [7] K. Champion, P. Zheng, A. Y. Aravkin, S. L. Brunton, and J. N. Kutz, A Unified Sparse Optimization Framework to Learn Parsimonious Physics-Informed Models From Data, *IEEE Access* **8**, 169259 (2020).
- [8] L. Boninsegna, F. Nüske, and C. Clementi, Sparse learning of stochastic dynamical equations, *The Journal of Chemical Physics* **148**, 241723 (2018).
- [9] T.-T. Gao and G. Yan, Autonomous inference of complex network dynamics from incomplete and noisy data, *Nature Computational Science* **2**, 160 (2022).
- [10] J. L. Callaham, J.-C. Loiseau, G. Rigas, and S. L. Brunton, Nonlinear stochastic modelling with Langevin regression, *Proceedings of the Royal Society A: Mathematical, Physical and Engineering Sciences* **477**, 20210092 (2021).
- [11] Y. Huang, Y. Mabrouk, G. Gompper, and B. Sabass, Sparse inference and active learning of stochastic differential equations from data, *Scientific Reports* **12**, 21691 (2022).
- [12] A. Nabeel, A. Karichannavar, S. Palathingal, J. Jhawar, D. B. Brückner, D. Raj M, and V. Guttal, Discovering stochastic dynamical equations from ecological time series data, *The American Naturalist* 10.1086/734083 (2024).
- [13] A. Frishman and P. Ronceray, Learning Force Fields from Stochastic Trajectories, *Physical Review X* **10**, 021009 (2020).
- [14] H. Risken, Fokker-Planck Equation for Several Variables; Methods of Solution, in *The Fokker-Planck Equation: Methods of Solution and Applications*, Springer Series in Synergetics, edited by H. Risken (Springer, Berlin, Heidelberg, 1996) pp. 133–162.
- [15] S. Siegert, R. Friedrich, and J. Peinke, Analysis of data sets of stochastic systems, *Physics Letters A* **243**, 275 (1998).
- [16] H. Risken, *The Fokker-Planck Equation: Methods of Solution and Applications*, edited by H. Haken, Springer Series in Synergetics, Vol. 18 (Springer, Berlin, Heidelberg, 1996).
- [17] P. Batz, A. Ruttor, and M. Opper, Approximate Bayes learning of stochastic differential equations, *Physical Review E* **98**, 022109 (2018).
- [18] H. Akaike, A new look at the statistical model identification, *IEEE Transactions on Automatic Control* **19**, 716 (1974).
- [19] É. Lebarbier and T. Mary-Huard, Une introduction au critère BIC : fondements théoriques et interprétation, *Journal de la société française de statistique* **147**, 39 (2006).
- [20] S. S. Wilks, The Large-Sample Distribution of the Likelihood Ratio for Testing Composite Hypotheses, *The Annals of Mathematical Statistics* **9**, 60 (1938).
- [21] G. Schwarz, Estimating the Dimension of a Model, *The Annals of Statistics* **6**, 461 (1978), 2958889.
- [22] K. Aho, D. Derryberry, and T. Peterson, Model selection for ecologists: The worldviews of AIC and BIC, *Ecology* **95**, 631 (2014), 43495189.
- [23] M. T. Brolly, J. R. Maddison, A. L. Teckentrup, and J. Vanneste, Bayesian comparison of stochastic models of dispersion, *Journal of Fluid Mechanics* **944**, A2 (2022).
- [24] A. A. Kaptanoglu, B. M. de Silva, U. Fasel, K. Kahe- man, A. J. Goldschmidt, J. Callaham, C. B. Delahunt, Z. G. Nicolaou, K. Champion, J.-C. Loiseau, J. N. Kutz, and S. L. Brunton, PySINDy: A comprehensive Python package for robust sparse system identification, *Journal of Open Source Software* **7**, 3994 (2022).
- [25] S. Amiri, Y. Zhang, A. Gerardos, C. Sykes, and P. Ronceray, Inferring geometrical dynamics of cell nucleus translocation, *Physical Review Research* **6**, 043030 (2024).
- [26] M. Wanner and I. Mezić, On Higher Order Drift and Diffusion Estimates for Stochastic SINDy, *SIAM Journal on Applied Dynamical Systems* **23**, 1504 (2024).
- [27] C. L. Vestergaard, P. C. Blainey, and H. Flyvbjerg, Optimal estimation of diffusion coefficients from single-particle trajectories, *Physical Review E* **89**, 022726 (2014).
- [28] S. Maddu, B. L. Cheeseman, I. F. Sbalzarini, and C. L. Müller, Stability selection enables robust learning of differential equations from limited noisy data, *Proceedings of the Royal Society A: Mathematical, Physical and Engineering Sciences* **478**, 20210916 (2022).
- [29] R. Tibshirani, Regression Shrinkage and Selection Via the Lasso, *Journal of the Royal Statistical Society Series B: Statistical Methodology* **58**, 267 (1996).
- [30] R. Ben Mhenni, S. Bourguignon, and J. Ninin, Global optimization for sparse solution of least squares problems, *Optimization Methods and Software* **37**, 1740 (2022).
- [31] N. M. Mangan, J. N. Kutz, S. L. Brunton, and J. L. Proctor, Model selection for dynamical systems via sparse regression and information criteria, *Proceedings of the*

Royal Society A: Mathematical, Physical and Engineering Sciences **473**, 20170009 (2017).

- [32] D. B. Brückner, P. Ronceray, and C. P. Broedersz, *Infering the Dynamics of Underdamped Stochastic Systems*, *Physical Review Letters* **125**, 058103 (2020).
- [33] Y. C. Mathpati, T. Tripura, R. Nayek, and S. Chakraborty, *Discovering stochastic partial differential equations from limited data using variational Bayes inference*, *Computer Methods in Applied Mechanics and Engineering* **418**, 116512 (2024).
- [34] H. Akaike, *Information Theory and an Extension of the Maximum Likelihood Principle*, in *Selected Papers of Hirotugu Akaike*, edited by E. Parzen, K. Tanabe, and G. Kitagawa (Springer New York, New York, NY, 1998) pp. 199–213.
- [35] K. P. Burnham, D. R. Anderson, and D. R. Anderson, *Model Selection and Multimodel Inference: A Practical Information-Theoretic Approach*, 2nd ed. (Springer, New York, NY, 2010).
- [36] D. B. Brückner, N. Arlt, A. Fink, P. Ronceray, J. O. Rädler, and C. P. Broedersz, *Learning the dynamics of cell–cell interactions in confined cell migration*, *Proceedings of the National Academy of Sciences* **118**, e2016602118 (2021).
- [37] F. Ferretti, V. Chardès, T. Mora, A. M. Walczak, and I. Giardina, *Building General Langevin Models from Discrete Datasets*, *Physical Review X* **10**, 031018 (2020).
- [38] I. Rish and G. Grabarnik, *Sparse Modeling: Theory, Algorithms, and Applications* (CRC Press, Boca Raton, 2014).
- [39] M. R. Leadbetter, G. Lindgren, and H. Rootzén, *Asymptotic Distributions of Extremes*, in *Extremes and Related Properties of Random Sequences and Processes*, edited by M. R. Leadbetter, G. Lindgren, and H. Rootzén (Springer, New York, NY, 1983) pp. 3–30.

## APPENDIX

### 1. Estimating the error $\mathcal{E}$ from the log-likelihood

We prove here Eq. 6 connecting the inference error  $\mathcal{E}(\hat{\mathbf{F}}^{\mathcal{B}})$  to the estimated log-likelihood  $\mathcal{L}(\mathbf{X}|\hat{\mathbf{F}}^{\mathcal{B}})$ . For simplicity, we assume here that the normalization matrix  $\bar{\mathbf{D}}$  is equal to the exact diffusion matrix  $\mathbf{D}$ , which has only a minor effect for non-multiplicative noise. We assume that  $\Delta t$  is small enough to write  $\Delta \mathbf{x}_t \approx \mathbf{F}(\mathbf{x}_t)\Delta t + \Delta \boldsymbol{\Xi}_t$  where  $\Delta \boldsymbol{\Xi}_t = \sqrt{2\mathbf{D}} \int_t^{t+\Delta t} \boldsymbol{\xi}(t) dt$ . By expanding the log-likelihood, we find

$$-\frac{4}{\tau} \mathcal{L}(\mathbf{X}|\hat{\mathbf{F}}^{\mathcal{B}}) = \left\langle \left( \mathbf{F} - \hat{\mathbf{F}}^{\mathcal{B}} \right) \cdot \mathbf{D}^{-1} \cdot \left( \mathbf{F} - \hat{\mathbf{F}}^{\mathcal{B}} \right) \right\rangle + \frac{2}{\Delta t} \left\langle \left( \mathbf{F} - \hat{\mathbf{F}}^{\mathcal{B}} \right) \cdot \mathbf{D}^{-1} \cdot \Delta \boldsymbol{\Xi}_t \right\rangle + \underbrace{\frac{1}{\Delta t^2} \left\langle \Delta \boldsymbol{\Xi}_t \cdot \mathbf{D}^{-1} \cdot \Delta \boldsymbol{\Xi}_t \right\rangle}_C$$

where  $C$  is model-independent and thus irrelevant for model comparison. We have  $\mathbb{E} \left[ \left\langle \mathbf{F} \cdot \mathbf{D}^{-1} \cdot \Delta \boldsymbol{\Xi}_t \right\rangle \right] = 0$ , while the term  $\left\langle \hat{\mathbf{F}}^{\mathcal{B}} \cdot \mathbf{D}^{-1} \cdot \Delta \boldsymbol{\Xi}_t \right\rangle$  requires more care.

Applying the Itô isometry:

$$\mathbb{E} \left[ \frac{2}{\Delta t} \left\langle \hat{\mathbf{F}}^{\mathcal{B}} \cdot \mathbf{D}^{-1} \cdot \Delta \boldsymbol{\Xi}_t \right\rangle \right] \approx \mathbb{E} \left[ \frac{4}{\tau} \sum_{i,j} (G_{\mathcal{B}}^{-1})_{ij} \left\langle \mathbf{b}_i \cdot \mathbf{D}^{-1} \cdot \mathbf{b}_j \right\rangle \right] = 4 \frac{n_{\mathcal{B}}}{\tau}.$$

where we neglected correlations between  $\mathbf{G}_{\mathcal{B}}^{-1}$  and  $\Delta \boldsymbol{\Xi}_t$  because they lead to higher-order terms. Consequently,

$$\mathbb{E} \left[ -\mathcal{L}(\mathbf{X}|\hat{\mathbf{F}}^{\mathcal{B}}) \right] = \tau \mathbb{E} \left[ \mathcal{E}(\hat{\mathbf{F}}^{\mathcal{B}}) \right] - n_{\mathcal{B}} + \mathbb{E}[C] \quad (10)$$

which straightforwardly leads to Eq. 6. Using log-likelihood differences to estimate the error difference between models thus favors over-parameterized models.

### 2. Statistics of the information gap $\Delta \mathcal{I}^*$

Here, we study the distribution of  $\Delta \mathcal{I}^*$  and prove its asymptotic Gumbel distribution (Eq. 8). We use the following result from (Ref. [39], example 1.7.4): for  $N$  independent, identically distributed Gaussian random variables  $X_1 \dots X_N \sim \mathcal{N}(0, 1)$ , we have  $P(\max(X_1^2, \dots, X_N^2) \leq z) = \exp(-e^{-(z-2\log(N))/2})$  to leading order when  $N \rightarrow \infty$ . Since each of the  $n_0 - n^*$  variables  $\Delta \mathcal{I}_s \sim \frac{1}{2} \chi_1^2$ , and assuming their independence, we can apply the previous results to obtain an approximate cumulative distribution function of  $\Delta \mathcal{I}^*$  (Eq. 8).

Note that, with the hypothesis of independence between  $\mathcal{I}_s$ , we can go beyond this result to obtain the exact cumulative distribution function

$$P(\Delta \mathcal{I}^* < z) = \text{erf}(\sqrt{z})^{n_0 - n^*} \quad (11)$$

(pink dashed line in Fig. 2d), allowing for more refined estimation of the information gap.

### 3. The parameter $p$ in $\mathcal{I}_{\text{PASTIS}}$

Here, we show that  $p$ , present in  $\mathcal{I}_{\text{PASTIS}}(\mathcal{B})$  (Eq. 9), is the probability of selecting a model with one superfluous term which can be written as  $\mathbb{P}[\max_s \mathcal{I}_{\text{PASTIS}}(\mathcal{B}^* + \{s\}) > \mathcal{I}_{\text{PASTIS}}(\mathcal{B}^*)] \approx p$ . First, we recall that  $\max_s \mathcal{I}_{\text{PASTIS}}(\mathcal{B}^* + \{s\}) - \mathcal{I}_{\text{PASTIS}}(\mathcal{B}^*) = \Delta \mathcal{I}^* - \log \frac{n_0}{p}$ . From Eq. 8, we obtain:

$$\begin{aligned} \mathbb{P}[\Delta \mathcal{I}^* > \log \frac{n_0}{p}] &\approx 1 - \exp \left[ -\frac{p(n_0 - n^*)}{n_0} \right] \\ &\approx 1 - \exp[-p] \quad \text{with } n_0 \gg n^* \\ &\approx p \quad \text{with } p \ll 1 \end{aligned}$$

In the previous derivation, we replaced  $n_0 - n^*$  by  $n_0$ , and we also used the approximated cumulative distribution function. These approximations tend to over-penalize

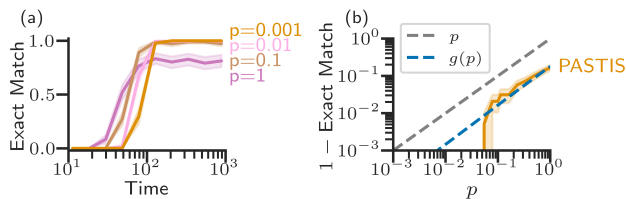


FIG. 5. **Influence of  $p$  on PASTIS** (a) Exact match accuracy for different value of  $p$  for a 10-dimensional Ornstein-Uhlenbeck as in Fig. 3b. (b) Asymptotic probability of identifying a wrong model against  $p$  for a long trajectory with  $\tau = 10^4$ . Blue dashed line: theoretical prediction  $g(p) = 1 - [\text{erf}(\log \frac{n_0}{p})^{\frac{1}{2}}]^{n_0 - n^*}$  for finite  $n_0$ .

complexity, as observed in Fig. 5b. A more precise penalization can be derived from the exact cumulative distribution function, leading to an accurate theoretical prediction of the exact match performance made by  $\mathcal{I}_{\text{PASTIS}}$  for long observation time (curve  $g(p)$  in (Fig. 5b). Increasing  $p$  thus increases probability of exact model recovery in the long trajectory limit, at the cost of needing more data to start identifying the model (Fig. 5a).

#### 4. Derivation of the Bayesian Information Criterion

The Bayesian Information Criterion (BIC), against which our method is benchmarked in Fig. 3, allows comparison of models in a Bayesian framework without having to select any particular prior  $\Pi_{\mathcal{B}}(F_1^{\mathcal{B}}, \dots, F_{n_{\mathcal{B}}}^{\mathcal{B}})$  on the parameters  $F_i^{\mathcal{B}}$ . Indeed, it gives the asymptotic form of the marginal likelihood  $P(\mathbf{X}|\mathcal{B})$  that is needed to obtain the posterior. We write from the marginal likelihood for the model associated to the base  $\mathcal{B}$ :

$$P(\mathbf{X}|\mathcal{B}) = \frac{1}{Z} \int e^{\mathcal{L}(\mathbf{X}|\mathbf{F}^{\mathcal{B}})} \Pi_{\mathcal{B}}(F_1^{\mathcal{B}}, \dots, F_{n_{\mathcal{B}}}^{\mathcal{B}}) dF_1^{\mathcal{B}} \dots dF_{n_{\mathcal{B}}}^{\mathcal{B}} \quad (12)$$

where  $\mathbf{F}^{\mathcal{B}} = \sum_i F_i^{\mathcal{B}} \mathbf{b}_i$ , and  $Z$  a  $F_i^{\mathcal{B}}$ -independent normalization constant. We Taylor-expand the likelihood (Eq. 3) around the maximizing parameters  $\hat{F}_i^{\mathcal{B}}$  of  $\mathcal{L}$ :

$$\mathcal{L}(\mathbf{X}|\mathbf{F}^{\mathcal{B}}) \approx \mathcal{L}(\mathbf{X}|\hat{\mathbf{F}}^{\mathcal{B}}) - \frac{\tau}{8} (\mathbf{F}^{\mathcal{B}} - \hat{\mathbf{F}}^{\mathcal{B}}) \cdot \mathbf{G}_{\mathcal{B}} \cdot (\mathbf{F}^{\mathcal{B}} - \hat{\mathbf{F}}^{\mathcal{B}}) \quad (13)$$

By also expanding the prior  $\Pi_{\mathcal{B}}$  around the maximizing parameters, injecting the previous result in Eq. 12 and computing the integral, we obtain:

$$P(\mathbf{X}|\mathcal{B}) \approx \frac{e^{\mathcal{L}(\mathbf{X}|\hat{\mathbf{F}}^{\mathcal{B}})}}{Z} \left( \frac{8\pi}{\tau} \right)^{\frac{n_{\mathcal{B}}}{2}} (\det \mathbf{G}_{\mathcal{B}})^{-\frac{1}{2}} \Pi_{\mathcal{B}}(\hat{\mathbf{F}}^{\mathcal{B}}) \quad (14)$$

In the long trajectory limit  $\tau \rightarrow \infty$ , we have  $(\det \mathbf{G}_{\mathcal{B}})^{-\frac{1}{2}} \Pi_{\mathcal{B}}(\hat{\mathbf{F}}^{\mathcal{B}}) = O(1)$ . By taking the log of the marginal likelihood, neglecting this  $O(1)$  term and model-independent constants, we find that the BIC can be defined as :

$$\text{BIC} = \mathcal{L}(\mathbf{X}|\hat{\mathbf{F}}^{\mathcal{B}}) - \frac{n_{\mathcal{B}}}{2} \log(\tau) \quad (15)$$

Thus, comparing models by comparing BIC values results, asymptotically for  $\tau \rightarrow \infty$ , in the same conclusion as comparing the marginal likelihood for any prior. We note that in most textbooks, BIC is defined with the log of the number of data points instead of the log of total time, which is problematic when  $\Delta t \rightarrow 0$ . Our definition is consistent with the observation in Ref. [13] that the information per unit time is bounded in Brownian dynamics.

#### 5. Addressing Data Imperfections

Large sampling intervals  $\Delta t$  and high measurement noise are two major challenges for both coefficient inference and model selection. We derive here modified estimators discussed in the main text and presented in Fig. 4. Both rely on a Stratonovich transformation of the stochastic sum  $\langle \frac{\Delta \mathbf{x}_t}{\Delta t} \cdot \bar{\mathbf{D}}^{-1} \cdot \mathbf{b}_j(\mathbf{x}_t) \rangle$  in the likelihood:

$$\mathcal{L}_{St.}^{\hat{\mathbf{D}}}(\mathbf{X}|\bar{\mathbf{F}}) = - \sum_{\alpha, \beta, \gamma} \frac{\tau}{2} \left\langle \hat{D}_{\gamma\beta}(\mathbf{x}_t) \frac{\partial \bar{F}_{\alpha}(\mathbf{x}_t)}{\partial x_{\beta}} \langle \hat{D} \rangle_{\gamma\alpha}^{-1} \right\rangle - \tau \left\langle \left( \left( \frac{\Delta \mathbf{x}_t}{\Delta t} - \frac{\bar{\mathbf{F}}(\mathbf{x}_{t+\Delta t}) + \bar{\mathbf{F}}(\mathbf{x}_t)}{2} \right) \frac{1}{\sqrt{4 \langle \hat{\mathbf{D}} \rangle}} \right)^2 \right\rangle \quad (16)$$

where we have explicit index summation in the first term, and  $\hat{\mathbf{D}}(\mathbf{x}_t)$  is an instantaneous diffusion estimator. Note that when  $\Delta t \rightarrow 0$  and  $\hat{\mathbf{D}}(\mathbf{x}_t) = \mathbf{D}(\mathbf{x}_t)$ , Eqs. 3 and 16 are equivalent. We now show how an adapted choice of  $\hat{\mathbf{D}}$  improves the robustness of the method.

##### a. Correcting large sampling intervals

When the sampling interval is large, we use a three-point estimator  $\hat{\mathbf{D}}_{\Delta t} = \frac{1}{4\Delta t} (\Delta \mathbf{x}_t - \Delta \mathbf{x}_{t-\Delta t}) \otimes (\Delta \mathbf{x}_t - \Delta \mathbf{x}_{t-\Delta t})$  which removes the leading-order drift-induced bias  $\mathbf{F}^2 \Delta t / 2$ . We complement this with a slight modification of the learned parameters:

$$\hat{F}_{\Delta t, i}^{\mathcal{B}} = \sum_j (G_{\mathcal{B}}^{\Delta t})_{ij}^{-1} \left\langle \frac{\Delta \mathbf{x}_t}{\Delta t} \cdot \langle \hat{\mathbf{D}}_{\Delta t} \rangle^{-1} \cdot \mathbf{b}_j(\mathbf{x}_t) \right\rangle \quad (17)$$

where  $(G_{\mathcal{B}}^{\Delta t})_{ij} = \left\langle \frac{(\mathbf{b}_i(\mathbf{x}_{t+\Delta t}) + \mathbf{b}_i(\mathbf{x}_t))}{2} \cdot \langle \hat{\mathbf{D}}_{\Delta t} \rangle^{-1} \cdot \mathbf{b}_j(\mathbf{x}_t) \right\rangle$  is a modified Gram matrix using trapezoid approximation, which has previously been shown to improve robustness of drift estimation to large time intervals [25, 26]. We thus define the information criterion used in Fig. 4a as  $\mathcal{I}_{\text{PASTIS}-\Delta t} = \mathcal{L}_{St.}^{\hat{\mathbf{D}}_{\Delta t}}(\mathbf{X}|\hat{\mathbf{F}}_{\Delta t}^{\mathcal{B}}) - n_{\mathcal{B}} \log \frac{n_0}{p}$ .

##### b. Correcting high measurement noise

We model measurement noise as  $\boldsymbol{\eta}_t \sim \mathcal{N}(\mathbf{0}, \sigma \mathbf{I})$  that additively impacts the observed trajectory  $\mathbf{x}_t \rightarrow$



$\mathbf{x}_t + \boldsymbol{\eta}_t$ . With classic estimators, this incurs  $O(\sigma^2/\Delta t)$  biases, which are a major hindrance to force inference. This leading-order bias vanishes when using the Stratonovich formulation of the log-likelihood due to statistically telescoping terms [13] in the stochastic sum  $\left\langle \frac{\Delta \eta_t}{\Delta t} \cdot \frac{\mathbf{F}^{\mathcal{B}}(\mathbf{x}_{t+\Delta t}) + \mathbf{F}^{\mathcal{B}}(\mathbf{x}_t)}{2} \right\rangle$ . We complement this with a corrected three-points estimator [27] of the diffusion matrix  $\hat{\mathbf{D}}_\sigma = \frac{1}{2\Delta t} \Delta \mathbf{x}_t \otimes \Delta \mathbf{x}_t + \frac{1}{\Delta t} \langle \Delta \mathbf{x}_{t+\Delta t} \otimes \Delta \mathbf{x}_t \rangle$ . Then, by maximizing  $\mathcal{L}_{St.}^{\hat{\mathbf{D}}_\sigma}$ , we obtain the learned parameters:

$$\hat{F}_{\sigma,i}^{\mathcal{B}} = \sum_j (G_{\mathcal{B}}^\sigma)_{ij}^{-1} \left( \left\langle \frac{\Delta \mathbf{x}_t}{\Delta t} \cdot \langle \hat{\mathbf{D}}_\sigma \rangle^{-1} \cdot \frac{\mathbf{b}_j(\mathbf{x}_t) + \mathbf{b}_j(\mathbf{x}_{t+\Delta t})}{2} \right\rangle - \sum_{\alpha,\beta,\gamma} \left\langle (\hat{D}_\sigma(\mathbf{x}_t))_{\gamma\beta} \frac{\partial b_{j,\alpha}(\mathbf{x}_t)}{\partial x_\beta} \langle \hat{D}_\sigma \rangle_{\gamma\alpha}^{-1} \right\rangle \right) \quad (18)$$

with  $(G_{\mathcal{B}}^\sigma)_{ij} = \left\langle \mathbf{b}_i(\mathbf{x}_t) \cdot \langle \hat{\mathbf{D}}_\sigma \rangle^{-1} \cdot \frac{\mathbf{b}_j(\mathbf{x}_{t+\Delta t}) + \mathbf{b}_j(\mathbf{x}_t)}{2} \right\rangle$ . This estimator is closely related to the one previously introduced in Ref. [13]. We finally define the information criterion  $\mathcal{I}_{\text{PASTIS}-\sigma} = \mathcal{L}_{St.}^{\hat{\mathbf{D}}_\sigma}(\mathbf{X}|\hat{\mathbf{F}}_\sigma^{\mathcal{B}}) - n_B \log \frac{n_0}{p}$ . Its minimization leads to the result presented in Fig. 4b.

Note that correcting simultaneously for large  $\Delta t$  and measurement noise is a substantial challenge for diffusion estimation, and thus for likelihood estimation and model inference.

## 6. Sparse inference of stochastic partial differential equations

We discuss here the adaptation of our information criterion  $I_{\text{PASTIS}}$  to Stochastic Partial Differential Equations (SPDEs) that we used in Fig. 3d. We consider a two-dimensional field  $\phi(x, y, t)$  that follows:

$$\frac{\partial \phi(x, y, t)}{\partial t} = F[\phi] + \sqrt{2D} \boldsymbol{\xi}(t, x, y) \quad (19)$$

where  $F[\phi]$  is the force functional, and for simplicity we take  $\boldsymbol{\xi}$  to be an additive Gaussian white noise with  $\mathbb{E}[\xi_\alpha(t, x, y)\xi_\beta(t', x', y')] = \delta(t-t')\delta(x-x')\delta(y-y')\delta_{\alpha\beta}$ . We consider a discretized trajectory in space and time  $\boldsymbol{\Phi} = \{\phi(t_i, x_j, y_k)\}_{(t_i=0,\dots,\tau), (x_j=0,\dots,L_x), (y_k=0,\dots,L_y)}$ . We adapt our trajectory average notation to fields with  $\langle \cdot \rangle = \frac{1}{\tau L_x L_y} \sum_{t_i, x_j, y_k} \cdot \Delta t \Delta x \Delta y$  where  $L_x, L_y$  are spatial

dimensions of the observed system. The log-likelihood is written for a test force functional  $\bar{\mathbf{F}}$ :

$$\mathcal{L}_{\text{SPDE}}(\boldsymbol{\Phi}|\bar{\mathbf{F}}) = \frac{-\tau L_x L_y}{4\bar{D}} \left\langle \left( \frac{\Delta \phi}{\Delta t} - \bar{\mathbf{F}} \right) \cdot \left( \frac{\Delta \phi}{\Delta t} - \bar{\mathbf{F}} \right) \right\rangle \quad (20)$$

where  $\bar{D} = \left\langle \frac{(\phi(t+\Delta t, x, y) - \phi(t, x, y))^2}{2\Delta t} \right\rangle$ . We approximate the true force field  $F$  using a linear combination of functionals  $\mathcal{B} = \{b_i[\phi]\}_{i=1\dots n_B}$ , such as polynomials and differential operators of  $\phi$ . We discretize these operators using simple finite differences:  $\frac{\partial \phi}{\partial x} = \frac{\phi(t_i, x_j + \Delta x, y_k) - \phi(t_i, x_j, y_k)}{\Delta x}$  and  $\frac{\partial^2 \phi}{\partial x^2} = \frac{\phi(t_i, x_j + \Delta x, y_k) - 2\phi(t_i, x_j, y_k) + \phi(t_i, x_j - \Delta x, y_k)}{\Delta x^2}$ . From the definition of the log-likelihood for SPDE (Eq. 20), the logic developed in the main text is transferable from SDE to SPDE. Thus, we define our information criterion  $I_{\text{PASTIS}}$  for SPDE as:  $I_{\text{PASTIS}}(\mathcal{B}) = \mathcal{L}_{\text{SPDE}}(\boldsymbol{\Phi}|\hat{\mathbf{F}}^{\mathcal{B}}) - \mathcal{L}_{\text{SPDE}}(\boldsymbol{\Phi}|0) - n_B \log \frac{n_0}{p}$  (Fig. 3d). Note that we have not studied the  $\Delta x \rightarrow 0$  limit here.

## 7. Simulations details and parameters

For all SDE and SPDE simulations, we use the Euler-Maruyama method with simulation time interval  $dt$  and sampling time interval  $\Delta t$ , and total simulation time  $\tau$ . For the prediction error in Fig. 3, we simulate a new independent trajectory with total time  $\tau_{\mathcal{E}}$ . Every trajectory is initiated using initial conditions obtained by simulating a trajectory for a total duration of  $\tau_{\text{therm.}} = 10$ , starting from a random initial state. For Lorenz simulations (Fig. 3a and Fig. 4), we use  $\sigma = 10, \rho = 28, \beta = 7/3, dt = 0.00002, \Delta t = 0.0002, D = 100, \tau_{\mathcal{E}} = 20$  and only for Fig. 4,  $\tau = 4 * 10^3$ . For each Ornstein-Uhlenbeck simulation, we choose a random  $\mathbf{A}$  (Fig. 3b1) with 1 on the diagonal and 10% of non-zero off-diagonal terms with 1 or -1 (Fig. 3b, Fig. 5). Then, we use  $dt = 0.001, \Delta t = 0.01, \tau = 10^4, \mathbf{D} = 100\mathbf{I}$  where  $\mathbf{I}$  is the identity matrix,  $\tau_{\mathcal{E}} = 10^3$ . For the Lotka-Volterra model, we define the matrix  $\mathbf{A}$  (Fig. 3c1) with -1 on the diagonal and 1 or -1 on the off-diagonal distributed as shown in Fig. 3c4. For simulations, we use  $dt = 0.001, \Delta t = 0.01, \tau = 10^4, D = 0.05, \tau_{\mathcal{E}} = 100$ . For the Gray-Scott model, we use  $D_u = 0.2097, D_v = 0.105, k = 0.057, F = 0.029$ . Then for simulations, we use a square lattice with periodic boundaries and discretized with  $dx = dy = \Delta x = \Delta y = 1$ , a length in space  $L_x = L_y = 100, dt = 0.001, \Delta t = 0.01, \tau = 50, D = 0.001, \tau_{\mathcal{E}} = 10$ .